

## Photodetachment of negative hydrogen ions

Meena P. Ajmera and Kwong T. Chung

*Department of Physics, North Carolina State University, Raleigh, North Carolina 27607*

(Received 24 February 1975)

The photodetachment cross section of the negative hydrogen ion is calculated for incident photon wavelengths in the range 1130 to 14040 Å. The free-state wave function of the bound-free transition is calculated from the simplified Kohn-Feshbach variational method. The bound-state wave function is given by Rotenberg and Stein, who used the Hylleraas correlated wave function with a "tail function" added to it. The agreement between the results from the length and velocity formulas in the present work is found to be considerably better compared to earlier theoretical results. The overall agreement with experimental results also shows some improvement. The cross section is found to rise and fall sharply in the closed-channel resonance region at the positions of the two singlet  $P$  resonances. The shape parameter  $q$  is also calculated for each resonance state.

### I. INTRODUCTION

The photodetachment of negative hydrogen ions is known to be one of the important causes of stellar opacity.<sup>1</sup> One of the earlier theoretical calculations carried out to determine the photodetachment cross sections of  $H^-$  was due to Chandrasekhar.<sup>2</sup> He derived three expressions for the photodetachment cross section known as dipole length, velocity, and acceleration formulas. The three expressions will give identical results if the bound- and free-state wave functions are exact. However, when approximate wave functions are used, the difference in the three results can provide a measure of consistency. Although close agreement between the results may not be inferred as the indication of reliable wave functions, large differences can almost always signify inferiority of the wave functions. This also means that the results are less likely to be reliable.

Many theoretical calculations have been carried out using this line of approach. For example, Geltman<sup>3</sup> has calculated cross sections using the 70-parameter Schwartz<sup>4</sup> wave function as well as the 20-parameter Hart-Herzberg<sup>5</sup> wave function for the bound state of  $H^-$  together with a variationally determined continuum function. Doughty *et al.*<sup>6</sup> have also investigated the process with the Schwartz bound state and a six-state close-coupling continuum function. More recently, Bell and Kingston<sup>7</sup> have calculated the absorption cross sections with the Schwartz bound-state function and a polarized-orbital continuum function.<sup>8</sup> A brief review of all the works associated with photodetachment of  $H^-$  is given by Risley.<sup>9</sup>

In none of the existing calculations do the results from length and velocity formulas fall very close to each other. For some incident wavelengths the discrepancy is found to be as much as 30%. A comparison with the experimental results of Smith

and Burch<sup>10</sup> reveals a significant difference between the theory and the experiment, especially for larger wavelengths.

The primary aim of the present work is twofold: first, to use improved bound- and free-state wave functions in order to reproduce the experimental results; second, to investigate the behavior of the cross section at those energies where closed-channel resonances occur. This has not been attempted in the previous calculations. In the earlier study of  $e^-$ -H elastic scattering, the singlet  $P$ -state wave function of  $H^-$  was accurately calculated using the simplified Kohn-Feshbach variational method.<sup>11-13</sup> The  $H^-$  bound-state wave function was obtained by adding to the usual Hylleraas wave-function<sup>14</sup> terms which express the correct asymptotic behavior. This wave function has been calculated by Rotenberg and Stein.<sup>15</sup> With a 33-parameter bound-state wave function they obtained an  $H^-$  ground-state energy of  $-0.5277499$  a.u. as compared to  $-0.5277475$  a.u. obtained by Schwartz using 70 parameters. Our calculation for the cross section gives better agreement between the results of the length and velocity formulas as compared to the previous results. The agreement with the experiment is also found to be somewhat better. In the closed-channel resonance region, a very steep rise and fall in the cross section is observed at the positions of both  $^1P$  resonances. The shape parameter<sup>16</sup>  $q$  is also calculated for each resonance state.

### II. WAVE FUNCTIONS AND CROSS SECTION FORMULAS

The usual theoretical description of photodetachment considers a negative ion interacting with an oscillating dipole electric field. The initial state is the ground state of  $H^-$  ion and the final state is a neutral hydrogen atom and a free electron. The photodetachment cross-section formulas are de-

rived by using time-dependent perturbation theory<sup>17</sup> and have the form

$$\sigma_L = 6.812 \times 10^{-20} k(k^2 + 2I) |\langle \Psi_F | (z_1 + z_2) | \Psi_B \rangle|^2 \text{ cm}^2, \quad (1)$$

$$\sigma_V = 2.725 \times 10^{-19} \frac{k}{k^2 + 2I} \left| \langle \Psi_F | \left( \frac{\partial}{\partial z_1} + \frac{\partial}{\partial z_2} \right) | \Psi_B \rangle \right|^2 \text{ cm}^2. \quad (2)$$

Equations (1) and (2) are more commonly referred to as the dipole length and velocity formulas, respectively.  $\Psi_B$  and  $\Psi_F$  represent the bound and free states of  $\text{H}^-$ ,  $k$  is the momentum (in a.u.) of the free electron, and  $I$  is the electron affinity of a neutral hydrogen atom (in a.u.). The wavelength of the incident photon is given by

$$\lambda = \frac{911.267}{k^2 + 2I} \text{ \AA}. \quad (3)$$

In the elastic scattering region, the ground state of neutral hydrogen is the only open channel. All the excited states of hydrogen are not assessible from the incident channel and hence they become closed channels. If we denote the projection operator onto the open channel by  $P$  and that for the closed channels by  $Q$ , the free-state wave function can be written as

$$\Psi_F = P\Psi_F + Q\Psi_F, \quad (4)$$

where

$$P\Psi_F = \Psi_{1s}(r_1)\Phi_p(r_2) + \Psi_{1s}(r_2)\Phi_p(r_1). \quad (5)$$

Here  $\Psi_{1s}$  is the ground state of hydrogen atom and  $\Phi_p$  is normalized to have the asymptotic form

$$\Phi_p(r) \xrightarrow{r \rightarrow \infty} 3i \cos \theta \cos \eta [j_1(kr) - \tan \eta n_1(kr)], \quad (6)$$

where  $\theta$  is the polar angle,  $\eta$  is the phase shift, and  $j_1$  and  $n_1$  are regular and irregular spherical Bessel functions, respectively. The closed-channel wave function is taken to be

$$Q\Psi_F = Q \left( \sum_{l=0} \sum_{m,n} \frac{1}{\sqrt{2}} (r_1^m r_2^n e^{-\beta r_1} e^{-\alpha r_2} |ll+110\rangle + 1 \leftrightarrow 2) \right), \quad (7)$$

where  $\alpha$  and  $\beta$  are nonlinear parameters to be optimized. The explicit forms of the operators and the wave functions along with the computational aspects are discussed in Refs. 12 and 13.

The bound-state wave function used in the present work was calculated by Rotenberg and Stein<sup>15</sup> and has the form

$$\Psi_B = \Psi_H + \Psi_T, \quad (8)$$

where  $\Psi_H$  is the Hylleraas wave function,

$$\Psi_H = \frac{A}{\pi\sqrt{8}} e^{-C(r_1+r_2)/2} \sum_{i,j,k} a_{ijk} (r_1+r_2)^i (r_1-r_2)^{2j} r_{12}^k. \quad (9)$$

Here  $a_{ijk}$  and  $C$  are variational parameters. In Eq. (8),  $\Psi_T$  is the "tail function" which asymptotically approaches the exact wave function:

$$\Psi_T = \frac{A}{2\pi} \left( e^{-r_1} \frac{e^{-sr_2} - e^{-tr_2}}{r_2} + 1 \leftrightarrow 2 \right). \quad (10)$$

The constant  $A$  in Eqs. (9) and (10) is referred to as the "tail coefficient" by Rotenberg and Stein.<sup>15</sup>

We have also used a simpler  $\text{H}^-$  bound-state wave function for cross-section calculations. This wave function includes full correlation in the angular part and has the form

$$\Psi_B = \sum_{i,j,l} C_{ijl} (r_1^i r_2^j e^{-\gamma r_1} e^{-\delta r_2} |ll00\rangle + 1 \leftrightarrow 2), \quad (11)$$

where  $\gamma$  and  $\delta$  are nonlinear parameters optimized to obtain the best ground-state energy value. The reason for carrying out the calculations with this wave function is discussed in the following section.

### III. RESULTS

The closed-channel part of the continuum wave function for the singlet  $P$  state of  $\text{H}^-$  contains four configurations namely,  $sp$ ,  $pd$ ,  $df$ , and  $fg$ . In calculating the dipole matrix elements with the correlated ground-state wave function, it was found that the computation becomes very involved if  $df$  and  $fg$  configurations are retained in the closed-channel wave function. Since these configurations make only a small contribution in the phase-shift calculation, it would be desirable to neglect this part of the wave function in the cross-section calculation. To justify this approximation, we use the simpler  $\text{H}^-$  bound-state wave function of Eq. (11) and observe the change in the cross section by gradually increasing the number of configurations in the wave function of Eq. (7). The simpler bound-state wave function used in this work contains 68 linear parameters and two nonlinear parameters. The ground-state energy of  $\text{H}^-$  obtained with this wave function has the value of  $-0.527447$  a.u. As expected, the agreement between length and velocity formulas is poor with the simpler bound-state wave function. The result is presented in Table I. It is clear from this table that in the wavelength range of interest, i.e. near 5280 \AA where the cross section is normalized to compare with the experiment and in the long-wavelength region,  $df$  and  $fg$  configurations contribute less than 1% to the cross section. It is also observed that higher configurations become more important as the energy of the incident photon approaches the inelastic threshold of hydrogen. However, in the closed-channel resonance region the closed-channel wave function we have used contains essentially  $sp$  and  $pd$  configurations, and hence the complete

TABLE I. The contribution to the photodetachment cross section (in units of  $10^{-17}$  cm $^2$ ) from different configurations of the wave function in Eq. (7). For the bound state of  $H^-$  the wave function given in Eq. (11) is used.

$k^2$ (a.u.)	$\lambda$ (Å)	$\sigma_L$ with number of configurations in $\Psi_F$			
		1	2	3	4
0.02	12 167	1.8051	1.7372	1.7433	1.7429
0.03	10 734	2.7739	2.6608	2.6709	2.6703
0.05	8687	4.0654	3.8714	3.8923	3.8888
0.08	6755	4.4966	4.2243	4.2546	4.2495
0.125	5065	3.6321	3.3223	3.3593	3.3518
0.16	4241	2.8337	2.5280	2.5653	2.5577
0.49	1672	1.0169	0.7451	0.7784	0.7707
0.64	1311	0.8014	0.5206	0.5503	0.5442

continuum wave function is used for this part of the cross-section calculation.

To investigate the convergence of cross section with respect to the correlated bound-state wave function, we have used three wave functions given by Rotenberg and Stein to calculate the cross sections with both length and velocity formulas. For the ground-state energy of  $H^-$ , they have obtained  $-0.527621$ ,  $-0.52773466$ , and  $-0.5277499$  a.u. with 5, 15, and 33 parameters, respectively, in the bound-state wave function. The results of the cross-section calculations are reported in Table II. At those wavelengths where the cross sections are relatively large, the three calculations differ at most by 2% or less. This difference increases to about 4% in the long wavelength region. We have also checked the convergence of the result with re-

spect to  $P\Psi_F$  by increasing the number of linear parameters in the wave function. No appreciable change in the result was observed.

The cross sections calculated with the 33-parameter  $H^-$  bound-state function using length and velocity formulas are plotted as a function of incident photon wavelength in Fig. 1. The results of the best previous calculations by Bell and Kingston<sup>7</sup> are also included in Fig. 1 along with the experimental points of Smith and Burch.<sup>10</sup> A comparison with the best results of Geltman<sup>3</sup> and with the results of Doughty *et al.*<sup>6</sup> and of Bell and Kingston<sup>7</sup> reveals that the overall agreement between the result of length and velocity formulas in the present work is better. More specifically, the maximum disagreement between the two results in the earlier calculations is over 20%, whereas it is about 8% in this work.

The relative merit of the length formula and the velocity formula has always been a controversial subject in the literature.<sup>18</sup> Since the length formula weighs the region far from the nucleus and velocity formula tends to emphasize the region closer to the nucleus, the relative accuracy of the results will largely depend on the system of interest as well as on how the approximated wave functions are obtained. For  $H^-$ , the binding energy is small and the system is loosely bound. Furthermore, the inclusion of tail function in the  $H^-$  ground state tends to make the wave function more accurate at large distances. Hence it is conceivable that the result of length formula in this work is more reliable than that of the velocity formula.

Experimentally, relative  $H^-$  photodetachment cross sections have been measured by Smith and

TABLE II. Calculated photodetachment cross sections (in units of  $10^{-17}$  cm $^2$ ) using correlated bound-state wave function with (I) 5 parameters, (II) 15 parameters, (III) 33 parameters.

$\lambda$ (Å)	$k^2$ (a.u.)	I		II		III	
		$\sigma_L$	$\sigma_V$	$\sigma_L$	$\sigma_V$	$\sigma_L$	$\sigma_V$
14 042	0.01	1.4544	1.4606	1.5582	1.4592	1.5314	1.4077
12 167	0.02	2.6882	2.7089	2.8500	2.7069	2.8096	2.6675
10 734	0.03	3.3963	3.4224	3.5645	3.4142	3.5246	3.4059
9603	0.04	3.7469	3.7662	3.8947	3.7378	3.8625	3.7181
8687	0.05	3.8731	3.8864	3.9894	3.8505	3.9677	3.8564
7931	0.06	3.8686	3.8738	3.9510	3.8330	3.9400	3.8601
7296	0.07	3.7881	3.7798	3.8385	3.7322	3.8375	3.7599
6755	0.08	3.6652	3.6489	3.6873	3.6008	3.6950	3.6415
6289	0.09	3.5199	3.4966	3.5182	3.4494	3.5332	3.4999
5883	0.10	3.3645	3.3367	3.3431	3.2919	3.3640	3.3510
5065	0.125	2.9782	2.9402	2.9243	2.9036	2.9549	2.9740
4241	0.16	2.4985	2.4503	2.4275	2.4225	2.4631	2.4813
2196	0.36	1.0901	1.0812	1.0731	1.0882	1.0941	1.1454
1672	0.49	0.7470	0.7558	0.7538	0.7638	0.7690	0.8166
1311	0.64	0.5544	0.5713	0.5703	0.5771	0.5838	0.6258

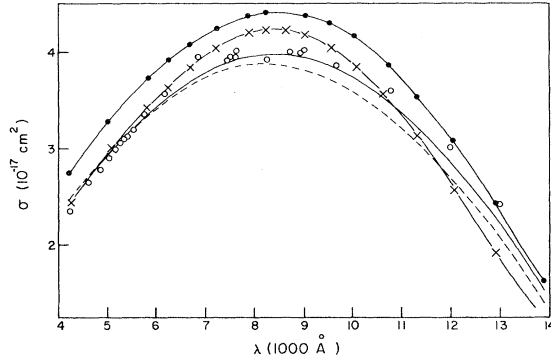


FIG. 1. Comparison of  $H^-$  photodetachment cross sections. Solid line, length curve and dashed line, velocity curve in the present work; crosses, length curve and closed circles, velocity curve obtained by Bell and Kingston; open circles, experimental points of Smith and Burch normalized to our length curve at 5280 Å.

Burch<sup>10</sup> with an estimated uncertainty of less than 3% assigned to each experimental measurement. These results were put on an absolute basis by Geltman<sup>3</sup> from the absolute integrated measurements of Branscomb and Smith,<sup>19</sup> with the value of  $3.28 \times 10^{-17} \text{ cm}^2$  at 5280 Å with an uncertainty of about  $\pm 10\%$ . Our value of cross section at 5280 Å is  $3.06 \times 10^{-17} \text{ cm}^2$  in the length formula and is in good agreement with the value obtained from absolute measurements. It is also in good agreement with the result of  $3.01 \times 10^{-17} \text{ cm}^2$  from the moment-adjusted method.<sup>20</sup> In Fig. 1, the experimental results are normalized to our length curve at 5280 Å for the purpose of comparison.

#### IV. CROSS SECTION AT RESONANCES

The Feshbach formalism<sup>21</sup> has given a firm theoretical ground to the closed-channel resonances. Earlier calculations have shown that there are two resonances for the  $^1P$  state of  $H^-$  in the elastic scattering region. The eigenvalues and eigenfunctions of  $QHQ$  operator for  $^1P$  state of  $e^-H$  system are calculated in Ref. 13. With the limited number of parameters in the wave function, the best eigenvalues have been obtained with only  $sp$  and  $pd$  configurations in the closed-channel segment of the trial function. The drastic rise and fall in the cross section is observed near the position of the two resonances. For example, near the first resonance, the cross section varies from 0 to  $3.104 \times 10^{-15} \text{ cm}^2$  where the background cross section is  $0.6 \times 10^{-17} \text{ cm}^2$ . Similarly for the sec-

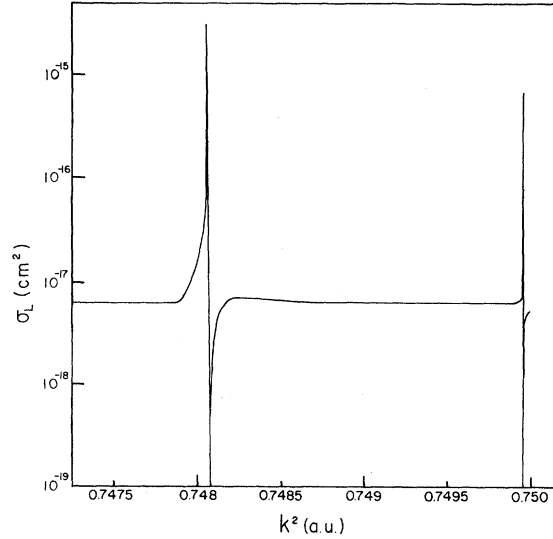


FIG. 2. Photodetachment cross sections of  $H^-$  near closed-channel resonances.  $k^2$  gives the momentum squared of the outgoing electron.

ond resonance, the cross section varies from 0 to  $6.59 \times 10^{-16} \text{ cm}^2$ . These results are shown in Fig. 2

To study the  $q$  parameter<sup>16</sup> which characterizes the line profile near a closed-channel resonance, we define

$$Q' = |\phi_n\rangle\langle\phi_n| \quad (12)$$

and

$$P' = 1 - Q', \quad (13)$$

where  $\phi_n$  is the eigenfunction of  $QHQ$  operator corresponding to eigenvalue  $\epsilon_n$ . The total continuum wave function can be written as

$$\Psi_F = \Psi_E^+ + \Lambda_n \frac{1}{E - P'HP'} P'H|\phi_n\rangle + \Lambda_n |\phi_n\rangle, \quad (14)$$

where  $\Psi_E^+$  is the solution of

$$(E - P'HP')\Psi_E^+ = 0 \quad (15)$$

and

$$\Lambda_n = \langle\phi_n|H|P'\Psi_F\rangle/(E - \epsilon_n). \quad (16)$$

The first term on the right-hand side of Eq. (14) represents the background continuum. The middle term arises from the interaction of  $|\phi_n\rangle$  with the continuum as well as with all the other  $\phi_j$ 's where  $j \neq n$ . This equation can be rewritten as

$$\Psi_F = e^{-i\gamma} \left[ \cos\gamma \Psi_E^+ + \sin\gamma \left( \mathcal{P} \int P'\Psi_\epsilon^+ \frac{\langle P'\Psi_\epsilon^+|H|\phi_n\rangle}{E - \epsilon} d\epsilon + |\phi_n\rangle \right) \right] / \pi \langle \Psi_E^+ | H | \phi_n \rangle \quad (17)$$

or

$$\Psi_F = e^{-i\gamma} [\cos\gamma \Psi_B^+ + \sin\gamma \Psi], \quad (18)$$

where

$$\tan\gamma = \frac{\Gamma_n/2}{E - \epsilon_n - \Delta_n}, \quad (19)$$

with  $\Gamma_n$  and  $\Delta_n$  being the width and shift, respectively, of a resonance state. Equation (18) has the same form as that derived by Fano except for the trivial phase factor. With the dipole-length operator as the transition operator for the photodetachment process,  $q$  can be defined as<sup>16</sup>

$$q = \frac{\langle \Psi | z_1 + z_2 | \Psi_B \rangle}{\langle \Psi_B^+ | z_1 + z_2 | \Psi_B \rangle}. \quad (20)$$

If we drop the phase factor in  $\Psi_F$ ,  $\Psi$  can be written as

$$\Psi = \frac{1}{\sin\gamma} \Psi_F - \cot\gamma \Psi_B^+. \quad (21)$$

Thus  $q$  becomes

$$q = \frac{1}{\sin\gamma} \frac{\langle \Psi_F | z_1 + z_2 | \Psi_B \rangle}{\langle \Psi_B^+ | z_1 + z_2 | \Psi_B \rangle} - \cot\gamma. \quad (22)$$

If we write  $\epsilon = \cot\gamma$ , the ratio of total cross section to the nonresonant cross section becomes

$$\frac{|\langle \Psi_F | z_1 + z_2 | \Psi_B \rangle|^2}{|\langle \Psi_B^+ | z_1 + z_2 | \Psi_B \rangle|^2} = \frac{(q + \epsilon)^2}{1 + \epsilon^2}. \quad (23)$$

$\Psi_F$  and  $\Psi_B^+$  have been calculated as described in Ref. 13, and hence  $q$  is obtained from Eq. (22) for each resonance state. We have calculated  $q$  at different energy values in the neighborhood of both resonances. We obtain  $q = -19.00$  for the lowest  $^1P$  resonance and  $q = -21.00$  for the second  $^1P$  resonance. However, the  $q$  value was found to vary by about  $\pm 0.03$  in the neighborhood of the first resonance and by  $\pm 0.15$  in the neighborhood of the second resonance.

The maxima and minima of  $\sigma(\epsilon)$  can be found immediately by differentiating Eq. (23) with respect to  $\epsilon$ . This gives a maximum at  $\epsilon = 1/q$  and a minimum at  $\epsilon = -q$ . Substituting this into Eq. (19), we find that the maximum in cross section occurs at

$$E = \epsilon_n + \Delta_n + \Gamma_n q / 2 \quad (24)$$

and the minimum at

$$E = \epsilon_n + \Delta_n - \Gamma_n / 2q. \quad (25)$$

The maxima and minima in the photodetachment cross section are shown in Fig. 2. Their positions are found to be in complete agreement with the predictions of Eqs. (24) and (25).

<sup>1</sup>L. H. Aller, *Astrophysics* (Ronald Press, New York, 1953), Vols. I and II.

<sup>2</sup>S. Chandrasekhar, *Astrophys. J.* **102**, 223 (1945); **102**, 395 (1945).

<sup>3</sup>S. Geltman, *Astrophys. J.* **136**, 935 (1962).

<sup>4</sup>C. Schwartz (unpublished).

<sup>5</sup>J. F. Hart and G. Herzberg, *Phys. Rev.* **106**, 79 (1957).

<sup>6</sup>N. A. Doughty, P. A. Fraser, and R. P. McEachran, *Mon. Not. R. Astron. Soc.* **132**, 255 (1966).

<sup>7</sup>K. L. Bell and A. E. Kingston, *Proc. Phys. Soc. Lond.* **90**, 895 (1967).

<sup>8</sup>A. Temkin and J. C. Lamkin, *Phys. Rev.* **121**, 788 (1961).

<sup>9</sup>J. S. Rissley, in *Atomic Physics IV. Proceedings of the Fourth International Conference on Atomic Physics, Heidelberg, 1974*, edited by G. zu Putlitz, E. W. Weber, and A. Winnacker (Plenum, New York, 1975).

<sup>10</sup>S. J. Smith and D. S. Burch, *Phys. Rev. Lett.* **2**, 165 (1959); *Phys. Rev.* **116**, 1125 (1959).

<sup>11</sup>K. T. Chung and J. C. Y. Chen, *Phys. Rev. Lett.* **27**, 1112 (1971).

<sup>12</sup>K. T. Chung and M. P. Ajmera, *Phys. Rev. A* **8**, 2895 (1973).

<sup>13</sup>M. P. Ajmera and K. T. Chung, *Phys. Rev. A* **10**, 1013 (1974).

<sup>14</sup>E. A. Hylleraas, *Z. Phys.* **48**, 469 (1928); **54**, 347 (1929).

<sup>15</sup>M. Rotenberg and J. Stein, *Phys. Rev.* **182**, 1 (1969).

<sup>16</sup>U. Fano, *Phys. Rev.* **124**, 1866 (1961); J. W. Cooper and U. Fano, *Phys. Rev.* **137**, A1364 (1965).

<sup>17</sup>L. I. Schiff, *Quantum Mechanics* (McGraw-Hill, New York, 1955).

<sup>18</sup>M. Cohen and R. P. McEachran, *Can. J. Phys.* **50**, 1363 (1973); *Chem. Phys. Lett.* **14**, 201 (1972); P. Jennings and E. B. Wilson, Jr., *J. Chem. Phys.* **47**, 2130 (1967); A. Dalgarno and J. T. Lewis, *Proc. Phys. Soc. Lond. A* **69**, 285 (1956); A. F. Starace, *Phys. Rev. A* **3**, 1242 (1971); *Phys. Rev. A* **8**, 1141 (1973).

<sup>19</sup>L. M. Branscomb and S. J. Smith, *Phys. Rev.* **98**, 1028 (1955).

<sup>20</sup>Y. K. Kim, Argonne National Laboratory Annual Report, 1966-1967, p. 30 (unpublished).

<sup>21</sup>H. Feshbach, *Ann. Phys. (N. Y.)* **5**, 357 (1958); **19**, 287 (1961).